A Color Constancy Model for Advanced Television Cameras

Po-Rong Chang *T. H. Hsieh* and *B. F. Yeh*

Dept. of Communication Engineering,
National Chiao-Tung University
Hsin-Chu, Taiwan

ABSTRACT

In high-fidelity color sensing, one may attempt to use recorded video image data from an electronic camcorder to generate a rendering that appears the same as the original image did at the time of acquisition. To achieve the goal, a color constancy mechanism is proposed to perceive the image color from the strengths of three RGB responses of a color camera or the like, indenpendent of the color of the light illuminating the object. Being able to extract the color descriptors that are independent of the illumination is desirable because of the varity of the situation in which color is important ,but illumination conditions cannot be controlled. The first step of our method is to use a finite dimensional linear model to estimate the color signals. We have shown that any color signal can be characterized as a linear combination of four principal component basis functions. Once the color signals have been estimated, the unknown illuminant can be determined by the Tominaga and Wandell's estimation method which is based on a dichromatic model. In color constancy, the knowledge of surface reflectance helps in determining the canonical color descriptors despite the variation in the spectral power distribution of the ambient light. It is shown that the estimate of surface reflectance is derived from both the estimated color signal and illuminant straightforwardly. The model of a combination of the estimations of the surface spectral reflectance and the color signals can be employed in designing a color constancy electronic video camera which indeed improves the shortcomings of the traditional video camcorders.

I. Introduction

Considerable experience has been gained by the worldwide use of the first gerneration HDTV cameras, for example, Sony's HDC-100, first introduced in 1984. Many program producers and lens manufacturers have made specific recommendations (primarily in the areas of camera sensitivity and system portability) in develpment of the second generation of HDTV cameras. More specifically, their suggestions included: improved sensitivity and extended dynamic range; improved image enhancement registration stability; and adherence to the emerging new SMPTE-240 M production standard [1]. The colorimetry of the camera has been modified to accommodate a wide color gamut specified by the SMPTE-240 M. Sony has addressed all of these areas by the development of the HDC-300 second generation HDTV tube camera [1].

In the area of CCD sensors for HDTV cameras [2], several manufacturers have announced the development of 2 million pixels CCD. The techonology of these devices is that of interline transfer. The Toshiba CCD chip of 25mm image size with 1920×1036 pixels claims to have an amorphous silicon photoconductive surface layer to improve sensitivity. Beside the functions of lightness constancy [15] for improving the quality and dynamic range of image acquisition, one would be likely to provide a high-fidelity color reproduction that appears the same as the object color appearance despite variation in the spectral power distribution of the ambient light. The color constancy mechanism is defined as the maintenance of color appearance that is independent of the color of the light illuminating the object.

In their early and important works on color constancy, Land and McCann [3] introduced an algorithm to perform color constancy, which they named the Retinex algorithm. This algorithm was based on the assumption that color information could be processed in three separate wavebands. More recent algorithms [4][5][6][7][8][9] have been investigated based on finite-dimensional linear models of surface reflectance or illuminant functions. These have either required that some form of spatial average of surface color be constant, or have required complex interaction between these functions. Wandell [4] and Maloney [8] started with the idea of describing color spectra with finite-dimensional linear models. The model condenses all spectral information into a few numbers by supposing that illumination and reflectance can each be approximated by weighted sums of basis functions. Making use of the relationship between receptor values and basis function weights, Wandell and Maloney showed how to recover both weights representing surface reflectance and those representing illumination. Another approach to render the correct colors of any color acquisition system under a variety of illuminant conditions is based on the color correction techniques [16][17]. They used eight correction matrices to compensate the actual scene illuminant and reduce the color error in the uniform CIE LUV color space. Hence, the color fidelity in video camera has been achieved under the standard light D_{65}.

In this paper, we consider a finite-dimensional approximation to the color signal and not approximations to surface spectral reflectance. It has been shown that any color signal can be expressed in terms of only four principal component functions. Therefore the weighting coefficients of the color signal representation can be determined by solving a set of equations based on the receptor values. In other words, the sensor measurements are transformed into an approximate linear model to the spectral power distribution of the light entering the camera. To achieve the recovery of perceived surface color descriptors which are independent of illuminant, the knowledge of surface spectral reflectance permits us to compute this canonical color constancy descriptors. Once the color signals have been identified, a procedure used to separate the color signal into the desired surface reflectance and illuminant is presented. Tominaga and Wandell [10] showed that the illuminant can be easily estimated based on the dichromatic reflection model for optically inhomogeneous materials. Since the objects in a scene may contain both optically homogeneous and optically inhomogeneous materials, a classification method is proposed to identify those materials. If there are more then two different inhomogeneous materials included in the scene, the illuminant is then computed by Tominaga and Wandell's method [10]. We have shown that Tominaga and Wandell's illuminant estimation method can be reformulated as solving a constrained least square error problem with a normalization equality constraint. Consequently, the surface reflectance is determined automatically. In the

[1]This work was supported in part by the National Science Council, Republic of China, under Contract NSC81-0404-E-009-027

0018-9316/92$03.00 © IEEE

last section, a number of typical test images are conducted to verify the proposed color constancy mechanism. It is found that the proposed method can recover the correct color descriptors under several lighting conditions.

II. Color Constancy Model

A color sensing device consists of a lens that focuses light reflected from an object onto a planar sensor array. The location of any object is identified with the location on the sensor array to which its image projects. The light arriving at array location $\mathbf{p}=(x,y)^T$ is called the color signal and denoted by $I(x,y,\lambda)$, where λ is visible wavelength and x and y are the spatial coordinates on the array, and T is the matrix transpose. The function $I(x,y,\lambda)$ specifies the quanta/second arriving at $\mathbf{p}$ at each wavelength λ across the electromagnetic spectrum. It is assumed to be a product of the ambient light $E(\lambda)$ and the surface spectral reflectance at $\mathbf{p}$, $S(x,y,\lambda)$. At any location in the object, the ambient light is specified by its spectral power distribution which describes the energy per second at each wavelength, λ or in units of quanta/sec. In this paper, the spectral power distribution of the light is assumed to be constant over a restricted region of the scene. The ambient light is reflected from surfaces and focused onto the sensor array. The proportion of light of wavelength λ reflected from object toward location $\mathbf{p}$ on the sensor array is determined by the surface spectral reflectance, $S(x,y,\lambda)$.

At each image location, we assume that there are L distinct classes of sensors corresponding to their associated sensor sensitivities. In video camera, there are three sensor classes, termed R, G, and B. This comes from color images obtained by taking pictures of the scene, through a red, a green, and a blue color filter. Each sensor quantum catch $Q_j(x,y)$, $j=1,2,...,L$, is of the form

$$\begin{aligned} Q_j(x,y) &= \int I(x,y,\lambda)q_j(\lambda)d\lambda \\ &= \int E(\lambda)S(x,y,\lambda)q_j(\lambda)d\lambda \end{aligned} \tag{1}$$

where $q_j(\lambda)$ is the jth sensor sensitivity and takes on only values between 0 and 1 inclusive. The information about the scene available to the visual system is contained in the L sensor quantum catches at each position $\mathbf{p}$. The spectral reflectance at each location $S(x,y,\lambda)$ is assumed to be unknown.

The color constancy problem usually means that the recovery of perceived surface color descriptor from the strengths of the three ($L=3$) sensors quantum catches representing the RGB responses of a color camera is independent of the light illuminating the object. In other words, color constancy attempts to provide color descriptors that are unaffected by changes in the illuminant and also predict the color appearance of the object under a canonical illuminant. Maloney [8] defines a canonical color descriptor which is a functional of $S(x,y,\lambda)$ and denoted by $\psi(S(x,y,\lambda))$. The functional ψ takes a function as argument and returns a single real number. An example of a canonical color desceiptor $\psi_j(S(x,y,\lambda))$ is

$$\begin{aligned} \psi_j(S(x,y,\lambda)) &= \int D_{65}(\lambda)S(x,y,\lambda)q_j(\lambda)d\lambda \\ j &= 1,2....,L \end{aligned} \tag{2}$$

where $D_{65}(\lambda)$ is a CIE standard source corresponding to normal daylight and has color temperature 6500^oK.

From (2), it is known that the knowledge of $S(x,y,\lambda)$ permits us to compute the canonical color descriptors that are independent of the ambient light $E(\lambda)$. Hence, the purpose of color constancy involves performing the inversion of equation (1), the recovery of the estimates of $S(x,y,\lambda)$ and the computation of the desired canonical color descriptors. The difficulty inherent in this approach is the mismatch between the amount of information available at the sensor array and the infinitely large number of parameters needed to fully specify each light and reflectance. To tackle this problem, [8] showed that equation (1) becomes invertible when both light and surface reflectance can be represented by a particular class of finite-dimensional linear models. Hence, the color constancy problem becomes solvable.

A. A Finite-Dimensional Representation for Color Signal

Over the visible spectrum (400nm-700nm), the surface spectral reflectance curves of natural objects are usually reasonably smooth and continuous. Many experiments on empirical surface spectral reflectances show that most of them can be modeled using only a few basis functions. For example, Cohen [5] found that over 99 percent of the variance of the spectral reflectance functions of the Munsell chips can be expressed using only three principal components. This analysis has been confirmed and extended by Maloney [8]. Higher dimensions result in better approximation, yet three functions still suffice when the filtering effect of the cone response functions is taken into account. The estimate of the surface spectral reflectance corresponding to position $(x,y)^T$ in the sensor array is expressed as

$$S(x,y,\lambda) = \sum_{i=1}^{3} \alpha_i(x,y)s_i(\lambda) \tag{3}$$

where $s_i(\lambda)$ is the ith basis function and $\alpha_i(x,y)$ is its associated position-dependent coefficient.

Consider approximating the spectral power distribution of light. Judd et al [6] reported that nearly all of the variations in the spectral power distribution of natural daylight can be described using a linear model consisting of three terms. This was confirmed in the later studies by Satri and Das as well as Maloney [8]. In addition, Maloney [8] has shown that the principal components that describe the observed variations in daylight and also describe the variations across another class of light source: the blackbody radiators. From these results, the spectral power distributions of lights can be characterized as

$$E(\lambda) = \sum_{j=1}^{3} \beta_j e_j(\lambda) \tag{4}$$

where $e_j(\lambda)$ is the jth basis function and β_j is its associated coefficient.

Hence, the color signal $I(x,y,\lambda)$ at a position in a sensory array can be expressed as a linear combination of nine functionals.

$$\begin{aligned} I(x,y,\lambda) &= \textstyle\sum_{i=1}^{3}\sum_{j=1}^{3}(\alpha_i(x,y)\beta_j)(s_i(\lambda)e_j(\lambda)) \\ &= \textstyle\sum_{i=1}^{3}\sum_{j=1}^{3}\rho_{ij}(x,y)\phi_{ij}(\lambda) \end{aligned} \tag{5}$$

where $\phi_{ij}(\lambda)=s_i(\lambda)e_j(\lambda)$ and $\rho_{ij}(x,y)=\alpha_i(x,y)\beta_j$.

In fact, the product terms $\phi_{ij}(\lambda)$ are not quaranteed to constitute a basis for $I(x,y,\lambda)$ even though $\{s_i(\lambda)\}$ and $\{e_j(\lambda)\}$ are basises for $S(x,y,\lambda)$ and $E(\lambda)$ respectively. Meanwhile $\{\phi_{ij}(\lambda)\}$ forms a spanning set for the Hilbert space of $I(x,y,\lambda)$. It is likely to reduce $\{\phi_{ij}(\lambda)\}$ to be a linearly independent spanning set by using singular value decomposition (SVD) technique. The SVD is a useful tool for orthogonal decomposition of general rectangular matrices. The application to data analysis is similiar to the idea of the well-known principal-component analysis. Let $\vec{\phi}_{ij}$ represent an n×1 column vector consisting n samples $\phi_{ij}(\lambda_k)$, $k=1,2,...,n$ over the visible spectrum (400nm - 700nm), that is, $\vec{\phi}_{ij}=[\phi_{ij}(\lambda_1),\phi_{ij}(\lambda_2),...,\phi_{ij}(\lambda_n)]^T$ where n is chosen to be larger than thirty practically. Hence one may use an n×9 sampling matrix $\mathbf{\Phi}=[\vec{\phi}_{11},\vec{\phi}_{12},...,\vec{\phi}_{33}]$ to describe the whole feature of $\{\phi_{ij}(\lambda)\}$. By performing the singular value decomposition on $\mathbf{\Phi}$, we have

$$\mathbf{\Phi} = U\Sigma V^T \tag{6.a}$$

or equivalently

$$\mathbf{\Phi} = \sigma_1\mathbf{u}_1\mathbf{v}_1^T + \sigma_2\mathbf{u}_2\mathbf{v}_2^T + ... + \sigma_9\mathbf{u}_9\mathbf{v}_9^T \tag{6.b}$$

where U(= $[\mathbf{u_1}, \mathbf{u_2}, ..., \mathbf{u_9}]$) and V(= $[\mathbf{v_1}, \mathbf{v_2}, ..., \mathbf{v_9}]$) are the n×9 left-hand singular matrix and the 9×9 right-hand singular matrix, respectively, and Σ is the 9×9 diagonal matix with elements of the singular values $\sigma_1, \sigma_2, ..., \sigma_9$. The n-dimensional left-hand singular vectors $\mathbf{u_1}, \mathbf{u_2}, ..., \mathbf{u_9}$ and 9-dimensional right-hand singular vectors $\mathbf{v_1}, \mathbf{v_2}, ..., \mathbf{v_9}$ are both orthonormal eigenvectors of $\mathbf{\Phi}\mathbf{\Phi}^T$ and $\mathbf{\Phi}^T\mathbf{\Phi}$ respectively. The singular values σ_i are the square roots of the eigenvalues of $\mathbf{\Phi}\mathbf{\Phi}^T$ and $\mathbf{\Phi}^T\mathbf{\Phi}$ and in descending order. [10] showed that a fairly reliable way to estimate the rank is to compare the singular values by using the following performance index:

$$R(k) = (\sum_{i=1}^{k} \sigma_i^2)/(\sum_{i=1}^{9} \sigma_i^2) \tag{7}$$

The approximate rank of $\mathbf{\Phi}$ is defined as the least integer of k's such that $R(k)$ is almost identical to one, i.e. , $\mid R(k) - 1 \mid \leq \epsilon$, where ϵ is a small positive number. The SVD of $\mathbf{\Phi}$ gave the singular values of $\sigma_1 = 2304.845$, $\sigma_2 = 722.428$, $\sigma_3 = 378.058$, $\sigma_4 = 131.211$, $\sigma_5 = 33.848$, $\sigma_6 = 13.614$, $\sigma_7 = 3.930$, $\sigma_8 = 2.271$, and $\sigma_9 = 1.340$, when n=31. The performance index was $R(1) = 0.8860$, $R(2) = 0.9730$, $R(3) = 0.9969$, and $R(4) = 0.9997$. The contributions of the remaining five components were negligibly small.

For this result, it can be found that the approximate rank of $\mathbf{\Phi}$ is almost identical to four. This implies that the spanning set $\{\phi_{ij}(\lambda)\}$ can be replaced by the first four principal component basis vectors which are the left-hand singular vectors $\mathbf{u_1}$, $\mathbf{u_2}$, $\mathbf{u_3}$, $\mathbf{u_4}$ and shown in Fig.1. It follows that the color signal $I(x, y, \lambda)$ can be expressed as

$$I(x, y, \lambda) = \sum_{k=1}^{4} \eta_k(x, y) u_k(\lambda) \tag{8}$$

where $u_k(\lambda)$ is the kth principal component basis function corresponding to $\mathbf{u_k}$ of $\mathbf{\Phi}$ and $\eta_k(x, y)$ is its associated coefficient. Substituting (8) into (1), it gets

$$Q_j(x, y) = \sum_{i=1}^{4} \eta_i(x, y) \omega_{ij} \tag{9}$$

where $\omega_{ij} = \int u_i(\lambda) q_j(\lambda) d\lambda$, $1 \leq i \leq 4, 1 \leq j \leq 3$
or eqivalently

$$\vec{Q}_{x,y} = W \vec{\eta}_{xy} \tag{10}$$

where $\vec{Q}_{xy} = [Q_1(x, y), Q_2(x, y), Q_3(x, y)]^T$ and $\vec{\eta}_{xy} = [\eta_1(x, y), \eta_2(x, y), \eta_3(x, y), \eta_4(x, y)]^T$ are 3×1 and 4×1 column vectors respectively. $W = [\omega_{ij}]$ is a 3×4 matrix. Since each sensor quantum catch $Q_j(x, y)$ at position $(x, y)^T$ is measurable and ω_{ij} are then computed, the unknown representation for $I(x, y, \lambda)$ can be determined by inverting equation (9) or (10). Then we have

$$\vec{\eta}_{xy} = W^+ \vec{Q}_{xy} \tag{11}$$

where W^+ is the Moore-Penrose generalized inverse [12].

III. General Color Reflection Model

The reflectance is devided into two parts: interface (specular) reflectance and body (diffuse or subsurface) reflectance [11]. The interface reflectance characterizes light reflection at the interface between the object's surface and the air. Reflection from optically homogeneous materials like metals and glasses is based mostly on this interface reflectance. Healey [11] showed that a unichromatic reflection model is a reasonable approximation for the homogeneous materials. For optically inhomogeneous materials like plastics and paints, the body reflectance becomes significantly. The body reflectance occurs for light that crosses the object's surface, and causes significant scattering among the pigment colorant layer. [11] used the Reichman body-scattering model to show that the dichromatic reflection

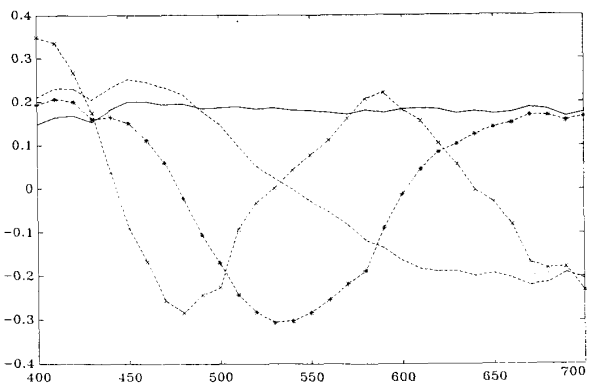

Fig1. The First Four Principal Components of Color Signal
"-"1st component "--"2nd component
"-*-"3rd component "-x-"4th component

model is a reasonable approximation for a large class of optically inhomogeneous materials. Although the surface spectral refletance varies with the illumination geometries of an object. The model suggests that the spectral reflectance is described as a weighted sum of two functions of the interface and body reflectances under all illumination geometries. Thus an approximate color reflectance model ($ACRM$) is proposed to combine the dichromatic reflection model for inhomogeneous dielectrics with a unichromatic reflectance model for homogeneous materials. The ACRM model is expressed in the form

$$I(x, y, \lambda) = \begin{cases} C_I(g) L_I(\lambda) & \text{for homo.} \\ C_I(g) L_I(\lambda) + C_B(g) L_B(\lambda) & \text{for inhomo.} \end{cases} \tag{12}$$

where g is a scene geometry function indicates dependence on the direction angle θ_d, the viewing angle θ_i, and the phase angle θ_p of the illumination geometry . By assuming a fixed mapping geometry, it can be shown that the scene geometry g is a function of image location $(x, y)^T$ at the sensor array [11]. $L_I(\lambda)$ and $L_B(\lambda)$ are the spectral power distributions of the interface and body reflection components, respectively. These components are unchanged as the geometric angles vary. The weights $C_I(g)$ and $C_B(g)$ are the geometric scale factors.

To express the ACRM model in terms of the surface reflectance functions, let $S_I(\lambda)$ and $S_B(\lambda)$ be the surface spectral reflectance for the two components of interface and body reflections, and let $E(\lambda)$ be the spectral power distribution of the incident light. Then the color signal at location $(x, y)^T$ in a sensor array is

$$I(x, y, \lambda) = \begin{cases} C_I(g) S_I(\lambda) E(\lambda) & \text{for homo.} \\ C_I(g) S_I(\lambda) E(\lambda) + C_B(g) S_B(\lambda) E(\lambda) & \text{for inhomo.} \end{cases} \tag{13}$$

and equivalently the total reflectance is described as

$$S(x, y, \lambda) = \begin{cases} C_I(g) S_I(\lambda) & \text{for homo.} \\ C_I(g) S_I(\lambda) + C_B(g) S_B(\lambda) & \text{for inhomo.} \end{cases} \tag{14}$$

The interface reflectance component $S_I(\lambda)$ is determined by Fresenel's law [11]. It is reported that many types of materials serving as vehicles in the surface layer are oil based and have constant refractive index. For these surfaces, the interface reflectance component becomes a constant over the visible wavelength.

A. Classfication of Materials

From equation (12), it is known that the color signal I(x,y,λ) can be expressed as a linear combination of the two component vectors $L_I(\lambda)$ and $L_B(\lambda)$ for the inhomogeneous materials or only a vector $L_I(\lambda)$ for homogeneous materials. For example, the two vectors $L_I(\lambda)$ and $L_B(\lambda)$ span a two-dimensional plane or subspace for the dichromatic model of the inhomogeneous materials. The spanned subspace containing all the possible color signals observed from an inhomogeneous surface is called the color-signal plane P. Similiarly, there exists a spanned one-dimensional color-signal plane for the unichromatic model of the homogeneous materials. Based on the above discussion, the classification of materials is dependent on the determination of the dimensionalities of their corresponding color-signal planes.

It is assumed that there are m color signals reflected from a region of the same material and arriving at m different image locations. Each color signal is sampled at n points over the visible wavelength. The m sampled color signals are represented by n-dimensional column vectors denoted by $\vec{I}_i = (I(x_i, y_i, \lambda_1), I(x_i, y_i, \lambda_2), ..., I(x_i, y_i, \lambda_n))^T$, where (x_i, y_i) is the image location for the *ith* color signal where 1 $\leq$ i $\leq$ m. Consequently, the m color signal vectors span a color signal plane P, and are summarized in an $n \times m$ observation matrix M defined by

$$M = [\vec{I}_1, \vec{I}_2, ..., \vec{I}_m] \tag{15}$$

The dimensionality of the space spanned by the measured color signals can be identified by the rank of the matrix M. Similiarly, one may use the singular performance index $R(k)=(\sum_{i=1}^{k} \sigma_i^2)/(\sum_{i=1}^{m} \sigma_i^2)$ defined in equation (7) to determine the rank of M, where σ_i is the *ith* singular value of the SVD of the matrix M. If $R(1) \cong 1.0$, then the measured data from an one dimensional color signal plane. In this case the observation conditions reveal only the interface reflections from the region. It can be concluded that the region contains the homogeneous material. If $R(2) \cong 1$, then the data generate a plane of dimensionality which is equal to two. Hence, the corresponding region contains the inhomogeneous material. For the case of data having a higher dimensionality than two, it can be concluded that the ACRM model is in error for this material.

B. Estimation of Illuminant and Surface Reflectances

More recently, Ho, Funt, and Drew [9] proposed a separation algorithm to extract the illuminant from a color signal. Unfortunately, it is found that their method is not very efficient. Another cost-effective approach to estimate the illuminant is proposed by Tominaga and Wandell [10]. They showed that the illuminant can be estimated based on the ACRM model. Here we would like to give a brief summary to describe their estimation method and reformulate it as a constrained least square error problem. It is known that the interface reflectance $S_I(\lambda)$ of many types of materials having oil-based surface layer is constant over the visible wavelenght. This implies that the interface spectral power distribution $L_I(\lambda)$ of the inhomogeneous materials depends on the illuminant $E(\lambda)$ only. In contrast to inhomogeneous materials, the interface reflectance of the homogeneous materials depends on the visible wavelength. Therefore, the illuminant cannot be extracted from the color signals for homogeneous materials. As consequence, each color signal plane for inhomogeneous material is spanned by the illuminant and body reflection. The illuminant corresponds to the intersection of two color signal planes for inhomogeneous materials. In other words, the scene should contain two or more inhomogeneous materials to provide an existance condition for determining the illuminant. Suppose that we measure color signals from the regions of two different inhomogeneous materials under the same light source. The color signals for these two regions can be described as follows:

$$I_1(x, y, \lambda) = C_{I1}(g)E(\lambda) + C_{B1}(g)S_{B1}(\lambda)E(\lambda) \tag{16.a}$$

and

$$I_2(x, y, \lambda) = C_{I2}(g)E(\lambda) + C_{B2}(g)S_{B2}(\lambda)E(\lambda) \tag{16.b}$$

The color signal planes $P(i)$ $(i = 1, 2)$ are constructed by a set of two vectors $E(\lambda)$ and $S_{Bi}(\lambda)E(\lambda)$. It is noted that illuminant vector is contained in both planes. Consequently, the process of extracting an illuminant spectrum can be reduced to be a computational problem of finding an intersection of two color signal planes. The intersection formulation can be extended to the case of three or more materials. All the planes must intersect at only a common line corresponding to the illuminant spectrum.

For the case of two inhomogeneous materials, The SVDs of the the observation matrices for both $P(1)$ and $P(2)$ become

$$M1 = U_1 \Sigma_1 V_1^T = \sigma_1^1 \mathbf{u_1^1 v_1^{1T}} + \sigma_2^1 \mathbf{u_2^1 v_2^{1T}} \tag{17.a}$$

and

$$M2 = U_2 \Sigma_2 V_2^T = \sigma_1^2 \mathbf{u_1^2 v_1^{2T}} + \sigma_2^2 \mathbf{u_2^2 v_2^{2T}} \tag{17.b}$$

Since the left-hand singular vector $\mathbf{u_1^i}$ and $\mathbf{u_2^i}$ are a set of basis vectors that span a two-dimensional color signal plane $P(i)$. Therefore, any color signal $I(i)$ belonging to $P(i)$ is expressed in a linear combination of $\mathbf{u_1^i}$ and $\mathbf{u_2^i}$

$$I(i) = \xi_1^i \mathbf{u_1^i} + \xi_2^i \mathbf{u_2^i} \tag{18}$$

Since the intersection line must lie in both $P(1)$ and $P(2)$, we have the relation

$$\xi_1^1 \mathbf{u_1^i} + \xi_2^1 \mathbf{u_2^1} = \xi_1^2 \mathbf{u_1^2} + \xi_2^2 \mathbf{u_2^2} \tag{19}$$

To solve ξ_i^j, $1 \leq i, j \leq 2$, the above equation should be rewritten as a homogeneous linear system

$$\Lambda \vec{\tau} = \mathbf{0} \tag{20}$$

where $\Lambda = [\mathbf{u_1^1}, \mathbf{u_2^1}, \mathbf{u_1^2}, \mathbf{u_2^2}]$ =an $n \times 4$ matrix and $\vec{\tau}=[\xi_1^1, \xi_2^1, -\xi_1^2, -\xi_2^2]^T$.

Next, we would introduce the following useful lemma which uses the concept of rank to characterize the solvability of equation (20).

Lemma1: Solvability of Equations [12]

Consider the system of equations $\mathbf{Ax} = \mathbf{b}$. The system is solvable if the rank of augmented matrix $[\mathbf{A}|\mathbf{b}]$ equals that of $\mathbf{A}$. Moreover, the system has infinitely many solutions when the rank is strictly less than the number of unknowns.

Since $\mathbf{b} = \mathbf{0}$ in equation (20), the rank of augmented matrix is always equal to that of $\mathbf{A}$. Furthermore, it is known that the augmented matrix $\Sigma = [\Lambda|\mathbf{0}]$ is derived by a sequence of elementary row operations from the $n \times 5$ matrix $\hat{\Omega} = [\vec{E}, S\vec{E}_1, \vec{E}, S\vec{E}_2, |\mathbf{0}]$, where $\vec{E} = [E(\lambda_1), E(\lambda_2), ..., E(\lambda_n)]^T$, $S\vec{E}_1 = [S_{B_1}(\lambda_1)E(\lambda_1), S_{B_1}(\lambda_2)E(\lambda_2), ..., S_{B_1}(\lambda_n)E(\lambda_n)]^T$ and $S\vec{E}_2=[S_{B_2}(\lambda_1)E(\lambda_1), S_{B_2}(\lambda_2)E(\lambda_2), ..., S_{B_2}(\lambda_n)E(\lambda_n)]^T$.

Hence the ranks of both augmented matrices are indentical. Looking upon the augmented matrix $\hat{\Omega}$, one may find that there are only three linearly indenpendent column vectors. Therefore, the rank of Σ is strictly less then the number of unknowns. From Lemma 1, it is concluded that equation (20) has infinitely many solutions.

By applying the constrained least-square-error technique to equation (20), the solution for $\vec{\tau}$ can be computed as

$$\min_{\vec{\tau}} \|\Lambda\vec{\tau}\| \quad subject \quad to \quad \|\vec{\tau}\| = 1 \tag{21}$$

where $\|\vec{\tau}\| = 1$ is the normalization constraint used to yield a unique solution of equation (20).

It is found in appendix 1 that the solution $\vec{\tau}$ is identical to the minimum eigenvector of $\Lambda^T\Lambda=\vec{\tau}^{min}$. Consequently, the estimate of illuminant is given by

$$\hat{E} = \tau_1^{min}\mathbf{u_1^1} + \tau_2^{min}\mathbf{u_2^1} \quad (22.a)$$

or

$$\hat{E} = -(\tau_3^{min}\mathbf{u_1^2} + \tau_4^{min}\mathbf{u_2^2}) \quad (22.b)$$

where τ_i^{min} is the ith component of $\vec{\tau}^{min}$.

It should be noted that that the method of estimating the illuminant is also true when the scene contains more than two inhomogeneous materials. Once the spectral power distribution of illumination is identified, the remainder of the problem is straightforward. The estimate of total surface reflectance at $(x,y)^T$ can then be computed using

$$\begin{aligned}\hat{S}(x,y,\lambda) &= \hat{I}(x,y,\lambda)/\hat{E}(\lambda) \\ &= \textstyle\sum_{i=1}^{4} \hat{\eta}_i(x,y)(u_i(\lambda)/\hat{E}(\lambda))\end{aligned} \quad (23)$$

where $\hat{I}(x,y,\lambda)$ is the estimated color signal and $\hat{\eta}_i(x,y)$ is the ith weighting coefficient.

IV. Experimental Results

A laboratory setup has been used to test the above algorithm. Color images are digitized using a Sony XC-711 CCD camera and gelatin filter. The camera is equipped with a primary color vertical stripe filter which gives color separation. Fig.2 illustrates the spectral sensitivity characteristics of the sensors. These curves have been taken from manufacture's specifications.

To demonstrate the effectiveness of the proposed color constancy method, a test pattern made of two different inhomogeneous materials, that is, yellow and brown NPL ceramic tiles with shadows, is particularly considered in our simulation. Assume that this test pattern is illuminated under two different typical light sources illuminant A and illuminant C which are defined in Wyszecki and Stiles [14]. Illuminant A and illuminant C are termed as the incandescent lamp and the correlated average daylight which have color temperatures 2854°K and 6770°K respectively. The images of test pattern taken under illuminant A and illuminant C are shown in Fig.6 and Fig.7 respectively. It is observed that the color appearances of both images seem quite different. To predict what an image would have looked like under a canonical illuminant D_{65}, the color signals at sensor array should be identified by performing equation (11) based on the sensor measurements. The estimated color signals at three typical sensor locations under illuminant A and illuminant C are shown in Fig.3.a and Fig.3.b respectively. For comparison, the dashed curves for the estimated color signals are approximately the same as the solid curves for the actual color signals. Next, one may use equation (22) to estimate the spectral power distributions of illuminant A and illuminant C. Both the estimated illuminants are shown in Fig.4.a and Fig.4.b. Finally, the resultant surface reflectances at three typical sensor locations derived from images under illuminant A and illuminant C are shown in Fig.5.a and Fig.5.b. As expected, the estimation method yields satisfactory approximations to the actual surface reflectances. Fig.8 and Fig.9 are the images of the color descriptors under the canonical illuminant D_{65} which are derived from the estimated surface reflectances of Fig.5.a and Fig.5.b respectively. For comparison, it turns out that the color appearances of both Fig.8 and Fig.9 are quite similar to that of the actual canonical color descriptor shown in Fig.10.

V. Conclusion

We have shown that any color signal can be characterized as a linear combination of four principal component basis functions. Hence the weighting coefficients of the color signal representation are identified by solving a system of equations based on the RGB responses of a color camera. Furthermore, it has indicated that the Tominaga and Wandell's illuminant estimation problem can be reformulated as solving a constrained least square error problem. Once both color signals and illuminant have been estimated, the surface reflectance is then computed automatically.

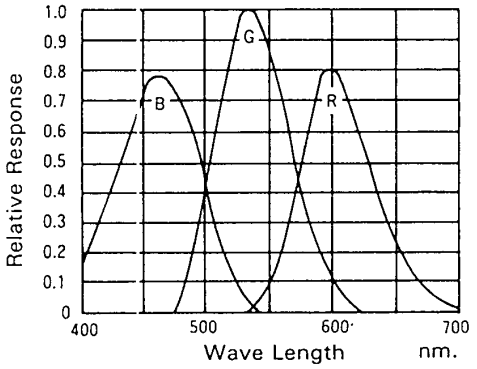

Fig.2 The spectral response curve of sensors of SONY Xc-711

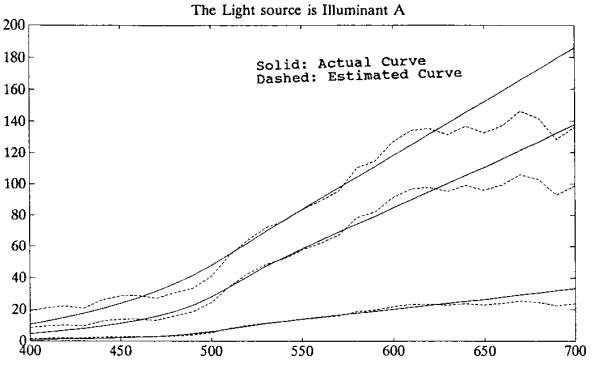

Fig3.a The estimated Color Signals of 3 typical sensor locations

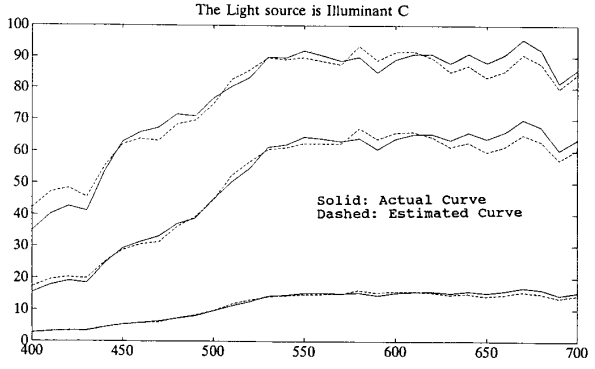

Fig3.b The estimated Color Signals of 3 typical sensor locations

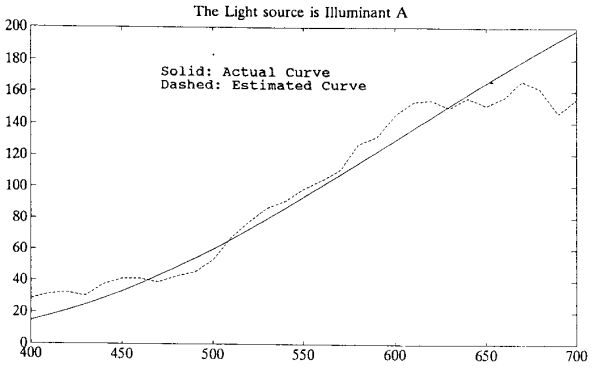

Fig4.a The Estimated SPD of Light Source

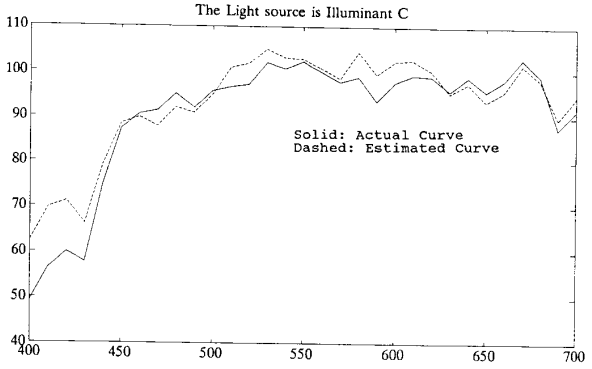

Fig4.b The Estimated SPD of Light Source

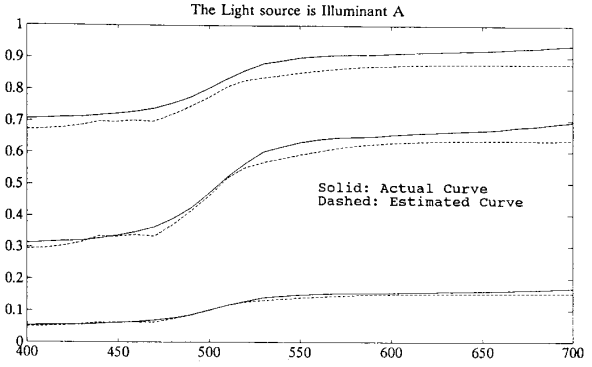

Fig5.a The estimated Reflectances of 3 typical sensor locations

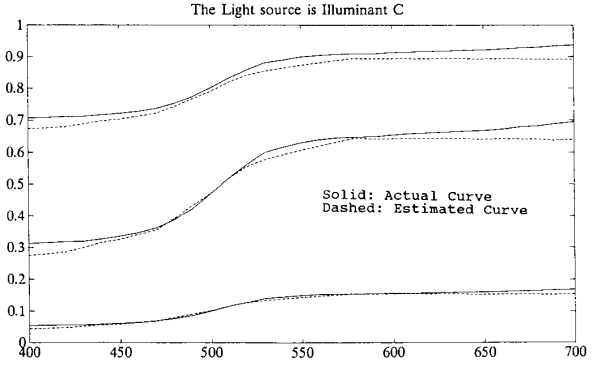

Fig5.b The estimated Reflectances of 3 typical sensor locations

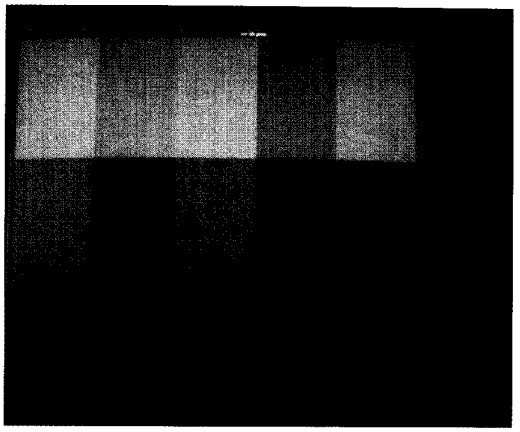

Fig.6 Image of test pattern under illuminant A

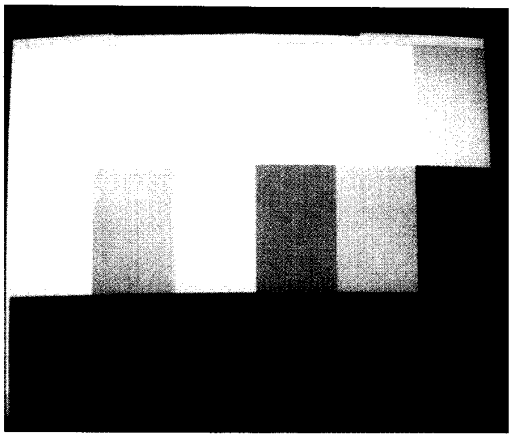

Fig.7 Image of test pattern under illuminant C

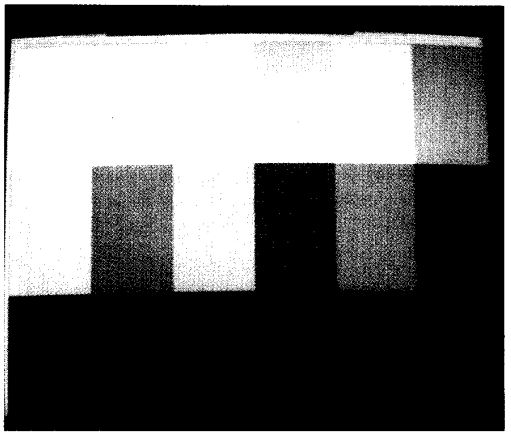

Fig.8 Image derived from Fig.5.a and under canonical D65

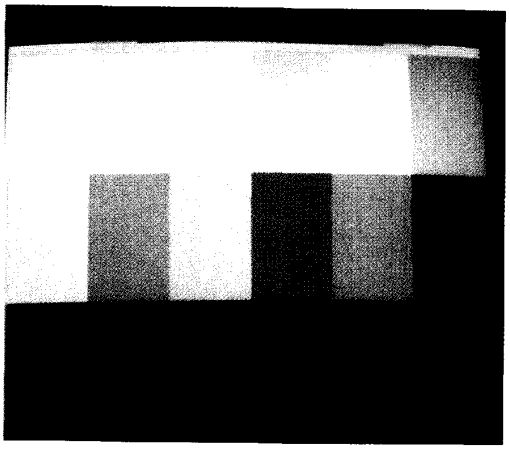

Fig.9 Image derived from Fig.5.b and under canonical D65

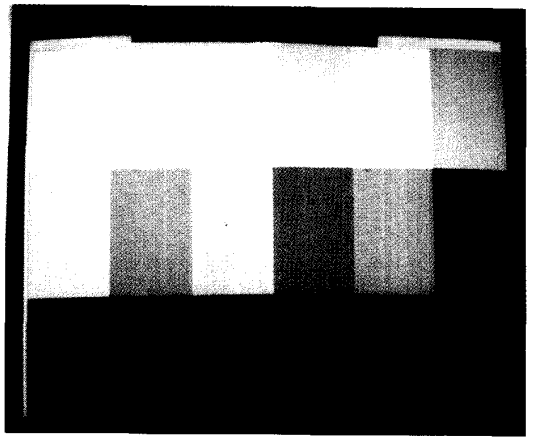

Fig.10 Image of the original test pattern under canonical illuminant D65

VI. Appendix 1

The solution to the constrained least square error problem of equation (21) can be found by using the following Lagrange multiplier formulation:

$$\min_{\vec{r}} \quad L(\vec{r},\lambda) = \|\Lambda\vec{r}\|_2^2 + \gamma(\|\vec{r}\|_2^2 - 1) \tag{A.1}$$

or equivalently

$$\min_{\vec{r}} L(\vec{r},\lambda) = \vec{r}^T\Lambda^T\Lambda\vec{r} + \gamma(\vec{r}^T\vec{r} - 1) \tag{A.2}$$

where γ is the Lagrange multiplier.

[12] shows that $\vec{r}^*$ is a relative minimum point for the problem of equation (21) if it satisfies the following Kuhn-Tucher conditions:

$$\nabla(\vec{r}^{*T}\Lambda^T\Lambda\vec{r}^*) + \gamma\nabla(\vec{r}^{*T}\vec{r}^* - 1) = 0 \tag{A.3}$$

and

$$\vec{r}^{*T}\vec{r}^* = 1 \tag{A.4}$$

or equivalently

$$(\Lambda^T\Lambda)\vec{r}^* = (-\gamma^*)\vec{r}^* = \lambda\vec{r}^* \tag{A.5}$$

It is shown that $\vec{r}^*$ and $\lambda = (-\gamma^*)$ are an eigenvector and an eigenvalue of $\Lambda^T\Lambda$ respectively. Substituting (A.4) and (A.5) into (A.2), we have

$$L(\vec{r}^*,\lambda) = \lambda \tag{A.6}$$

If $\vec{r}^*$ is chosen to have minimum eigenvalue λ_{min} such that $L(\vec{r}_{min},\lambda_{min}) \leq L(\vec{r}^*,\lambda)$ for all $\vec{r}^*$.

VII. REFERENCE

[1] Thorpe L. "Second-Generation HDTV Camera" SMPTE, Better Video Images, p170-p199, 1989.

[2] Poetsh D. " A Digital CCD Telecine for HDTV" Symposium Record, Broadcast Section, Montreux, June ,p113-p122, 1989.

[3] E. H. Land and J. J.McCann " Lightness and Retinex Theory", J. Opt. Soc. Am. 61, p1-p11, 1971.

[4] Brian A. Wandell "Color constancy and Natural Image", Phycica. Scripta. Vol.39, p187-p192, 1989.

[5] J.Cohen " Dependency of the spectral Reflectance Curves of Munsell Color Chip", Psychon. Sci. vol 1, p369-p370, Aug. 1964.

[6] D. B. Judd, D. L. MacAdam and G. Wyszecki " Spectral Distribution of Typical Daylight As a Function of Correlated Color Temperature" J. Opt. Soc. Am. vol 54, p1031-p1040, Aug. 1964.

[7] B. A. Wandell, "Color Rendering of Color Camera Data", Color Research and Application vol. 11, p30-p33, 1986.

[8] Maloney, Laurence Thomas "A Computational Approach to Color Constancy", Ph. D. Dissertation, Appl. Psychol. Lab. Stanford Univ. , Stanford, CA. 1985.

[9] Jian Ho, Brian V. Funt, and, Mark S. Drew, "Separating a Color Signal into Illuminant and Surface Reflectance Components:Theory and Application",IEEE Trans. on Pattern Recognition and Machine Intelligence, vol.12, p966-p77, 1990.

[10] Shoji Tominaga and Brian A. Wandell "Standard Surface- reflectance Model and Estimation", J. Optical Society of America, p576-p584, 1989.

[11] Glenn Healey" Using Color for Geometry-Insensitive Segmentation ", J. Optical Society of America, p920-p937, 1989.

[12] Ben Noble, James W. Daniel , Applied Linear Algebra, Third Edition, Prentice-Hall, 1988.

[13] D. G. Luenberger, Linear and Nonlinear Programming, Second Edition, Addison-Wesley Company, 1984.

[14] G. Wyszecki and W. S. Stiles, Color Science: Concept, and Methods, Qualitative Data and Formulate. John Wiley: New York, 1982.

[15] P. R. Chang and B. F. Yeh, "Retina-like Image Acquisition with Wide-Rage Light Adaptation", SPIE Visual Comm. and Iamge Processing, Vol.1606, P456-P469, Boston, MA, 1991.

[16] J.F. Monahan and R. A. Dischert, "Color Correct Techniques for Television Camera", Journal of the SMPTE, Vol. 78, P696-P700, Sept. 1969.

[17] R. J. Green and S. J. Ismail, "Color Error Reduction in Video Systems", IEEE Trans. on Broadcasting, Vol. 36, No.1, P99-P105, March, 1990.

Po-Rong Chang (M'87) received the B.S. degree in electrical engineering from the National Tsing-Hua University, Taiwan, in 1980, the M.S. degree in telecommunication engineering from National Chiao-Tung University, Hsinchu, Taiwan, in 1982, and the Ph.D. degree in electrical engineering from Purdue University, West Lafayette, IN, 1988.

From 1982 to 1984, he was a lecturer in the Chinese Air Force Telecommunication and Electronics School for his two-year military service. From 1984 to 1985 he was an instructor of electrical engineering at National Taiwan Institute of Technology, Taipei, Taiwan. From 1989 to 1990, he was a project leader in charge of SPARC chip design team at ERSO of Industrial Technology and Research Institute, Chu-Tung, Taiwan. Currently he is an Associate Professor of Communication Engineering at National Chiao-Tung University. His current interests include fuzzy neural network, HDTV color signal processing, and human visual and audio systems.

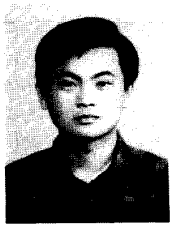

T. H. Hsieh was born in Taiwan in 1968. He received the B.S. degree and the M.S. degree in communication engineering from the National Chiao-Tung University Hsin-chu, Taiwan in 1990 and 1992 respectively. His current research insterests are in the area of HDTV color signal processing , fuzzy set theory and applications, and neural network.

B. F. Yeh was born in Taipei, Taiwan in 1965. He received B.S. degree in electronics engineering from Chung-Yung Christian University in 1989, the M.S. degree in communication engineering from the National Chiao-Tung University, Hsinchu, Taiwan, in 1991, where he currently pursuing the Ph.D. degree. His current research interests are in the area of fuzzy set theory and neural nerwork.